

# Pronounced Self-Induced Diastereomeric Anisochronism in Anisidine Amino Acid Diamides

Jan-Michael Menke<sup>[a]</sup> and Oliver Trapp<sup>\*[a]</sup>

The emergent properties resulting from selective supramolecular interactions are of significant importance for materials and chemical systems. For the directed use of such properties, a fundamental understanding of the interaction mechanism and the resulting mode of function is necessary for a tailored design. The self-induced diastereomeric anisochronism effect (SIDA), which occurs in the intermolecular interaction of chiral molecules, generates unique properties such as chiral

self-recognition and nonlinear effects. Here we show that anisidine amino acid diamides lead to extraordinary signal splitting in NMR spectra through supramolecular interaction and homochiral self-recognition. By systematic experiments we have investigated the underlying SIDA effect, explored its limits and finally successfully utilized it in the determination of enantiomeric ratios by NMR spectroscopy of chiral 'SIDA-inactive' compounds such as thalidomide.

## Introduction

The exploration of supramolecular systems enables a profound understanding of the chemical processes in living organisms, the origins of life and the possibility of developing machines at the molecular level.<sup>[1]</sup> There is enormous interest in this area of chemistry, which includes the development of temperature- or additive-controlled<sup>[2]</sup> and light-controlled molecular machines,<sup>[3]</sup> self-healing materials<sup>[4]</sup> and autoamplification.<sup>[5]</sup> Catenanes,<sup>[6]</sup> knots<sup>[7]</sup> and rotaxanes<sup>[8]</sup> can also be produced using this approach. In addition to naturally occurring helical DNA and RNA, synthetic supramolecular helices have also been investigated<sup>[9,13]</sup> and used for catalytic purposes.<sup>[14,16]</sup> Diastereoselective interactions<sup>[17,19]</sup> via foldamer units such as the selective recognition of dicarboxylic acids<sup>[20]</sup> and sugars<sup>[21,22]</sup> have been observed. In addition to the product-catalyst interaction,<sup>[23]</sup> catalyst dimerization<sup>[24,26]</sup> leads to a high enantioselectivity of the catalyzed reactions. Another supramolecular effect is known as the ESDA effect (enantioselective self-disproportionation on achiral phase) and is used in the separation of enriched enantiomeric mixtures without the use of a chiral stationary phase (CSP).<sup>[27,34]</sup> A related effect is the SIDA effect (self-induced diastereomeric anisochronism) by self-recognition of the enantiomers.<sup>[35]</sup> Without the addition of further chiral reagents such as (lanthanide) shift reagents or

chiral resolving reagents,<sup>[36,37]</sup> enantiomeric ratios (*ee*) can be monitored in NMR spectroscopy.<sup>[38,39]</sup> For the emergence of the SIDA effect, it is supposed that the formation of supramolecular transient dimer or multimer structures takes place.<sup>[40,42]</sup> Hydrogen bonds, but also  $\pi$ - $\pi$  stacking, play an important role here. Three-point interactions are also a well-established concept. Only a few examples have been reported so far: Perylene bisimides,<sup>[43]</sup> ruthenium complexes,<sup>[44]</sup> natural products,<sup>[45]</sup> carboxylic acids,<sup>[46]</sup> carboxamides,<sup>[47,50]</sup> 2,2-dibutyl-1,3,2-dioxastannolanes,<sup>[51]</sup> and 1,5-benzothiazepines.<sup>[52]</sup> We investigated alanine derivatives with the aim of using them as recognition units in self-recognizing and autoamplifying chiral ligands for asymmetric hydrogenations.<sup>[53]</sup> Alanine methyl esters are particularly interesting because they are the reaction product of methyl 2-acetamidoacrylates and lead to the alignment of the tropos ligand and catalyst when interacting with a recognition unit. Therefore, the aromatic electron-deficient derivative *N*-3,5-dinitrobenzoylalanine methyl ester was comprehensively investigated, which showed a pronounced SIDA effect. However, it was also evident that this system is still limited in its scope of application, i.e. the recognition of other chiral compounds.

In general, the SIDA effect can be used to rapidly determine the enantiomeric ratio (*ee*) of the product in catalytic transformations that are otherwise determined by HPLC or GC methods. In our research on self-amplifying catalysts,<sup>[54,55]</sup> we have identified anisidine-based amino acid diamides that exhibit remarkable SIDA effects. Therefore, we investigated and expanded the scope of this compound class and analyzed the limitation of the SIDA effect, with particular attention to optimal performance, mechanistic considerations, and potential applications. Here we present a systematic investigation of anisidine-based amino acid diamides, as these are of great value as potential recognition sites and supramolecular applications in general.

[a] Dr. J.-M. Menke, Prof. Dr. O. Trapp  
 Department of Chemistry  
 Ludwig-Maximilians-Universität München  
 Butenandtstr. 5–13  
 81377 Munich (Germany)  
 E-mail: oliver.trapp@cup.uni-muenchen.de

Supporting information for this article is available on the WWW under <https://doi.org/10.1002/chem.202400623>

© 2024 The Authors. Chemistry - A European Journal published by Wiley-VCH GmbH. This is an open access article under the terms of the Creative Commons Attribution Non-Commercial License, which permits use, distribution and reproduction in any medium, provided the original work is properly cited and is not used for commercial purposes.

## Results and Discussion

The synthetic preparation of chiral anisidine-based amino acid diamides starts from anisidine, which was converted via peptide coupling to the corresponding Boc-protected amino acid amide. Acid deprotection followed by reaction with pivaloyl chloride gives the corresponding enantiomerically pure diamide compounds in good yields (cf. Figure 1).

First of all, the influence of the methoxy group, which served as a spectroscopic probe, was investigated regarding the SIDA effect. The *ortho*-anisidine does not exhibit a SIDA effect, which we attribute to steric repulsion and/or interference with hydrogen bond formation by another acceptor in the spatial

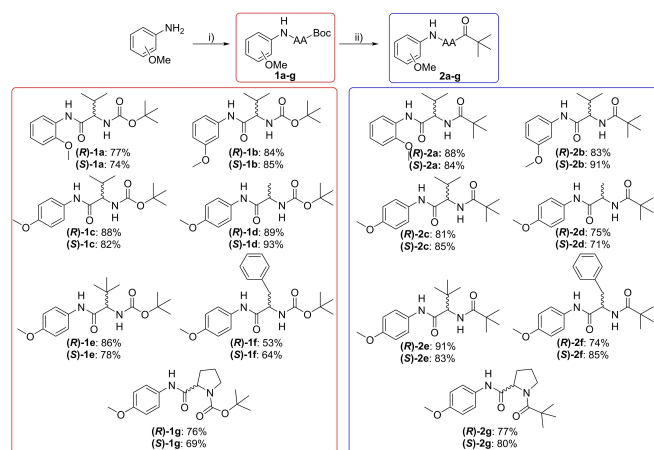


**Figure 1.** Synthesis of chiral anisidine amino acid diamides. Reaction conditions: i) Boc-AA-OH, COMU, DIPEA, DCM, 0 °C to rt; ii) HCl, iPrOH, CHCl<sub>3</sub>, then evaporation, followed by pivaloyl chloride, NEt<sub>3</sub>, DCM (AA = amino acid).

proximity of an amide group. This is in contrast to the meta- and para-substituted anisidine derivatives. They show a highly pronounced SIDA effect for both the <sup>1</sup>H and <sup>13</sup>C NMR signals. Figure 2 A demonstrates exemplarily splitting of the signals for the amide proton of anisidine.

The enantiomerically pure (*R*)-**2b** shows only one set of signals. Addition of the opposite enantiomer gives rise to another signal set. The ratio of the two signals correlates with the composition of the enantiomeric ratio. Further reduction of the enantiomer ratio leads not only to an increase in the area of the newly formed signal and a corresponding reduction of the original signal, but also to a decrease in the splitting until the signals coincide (ratios 90:10 to 50:50). If this procedure is carried out starting from the (*S*)-enantiomer, an identical result is obtained (ratios 10:90 to 50:50). For selected protons and carbon atoms, the applied enantiomeric excess was plotted against the splitting  $\Delta\delta$  (Figure 2 B). S-shaped in the ee-dependent chemical shifts was observed for all signals. This arises from the fact that the chemical shifts of the enantiomers in the dimeric aggregates are a function of the concentration and the relative energy stability of the dimers, which can be mathematically described by statistically weighted contributions of the homo- and hetero aggregates to the observed chemical shift.<sup>[56]</sup> Small differences in enantiomeric excess near the racemate have a particular strong impact on the size of the splitting.

With increasing enantiomeric excess this influence decreases. Apparently, *meta*-substitution of the methoxy group at the aromatic anisidine moiety leads to a partly pronounced enhancement of the SIDA effect. Decrease in the concentration leads to a lower splitting. The averaged shift difference of the enantiomer ratios 90:10 and 10:90 is given in Figure 2 C for all

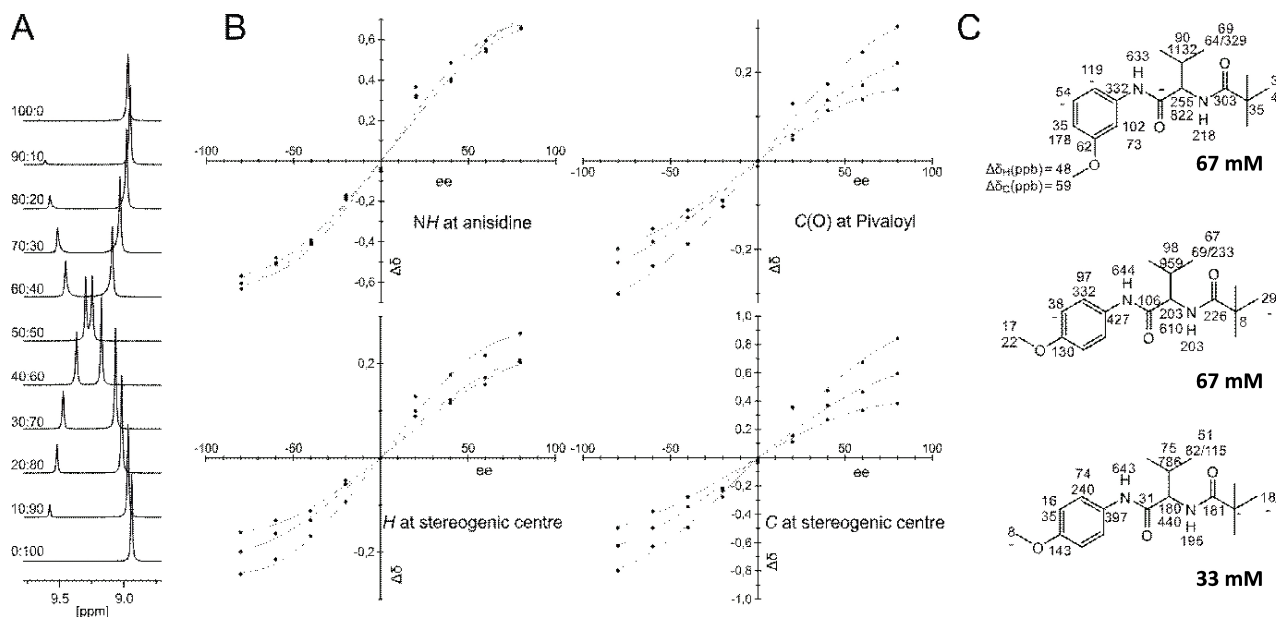


**Figure 2.** A: Stacked <sup>1</sup>H NMR spectra in the amide region of 2b with different enantiomeric ratios in CDCl<sub>3</sub> at room temperature (67 mM). B: S-shaped behavior for selected signals of *m*-NH(PivVal)anisidine 2b 67 mM (black), *p*-NH(PivVal)anisidine 2c 67 mM (red), *p*-NH(PivVal)anisidine 2c 33 mM (blue). C: Average splitting  $\Delta\delta$  of carbon (red) and proton (blue) signals at 90:10 and 10:90 enantiomeric ratio and concentrations of 33 mM and 67 mM, respectively, in CDCl<sub>3</sub> at room temperature.

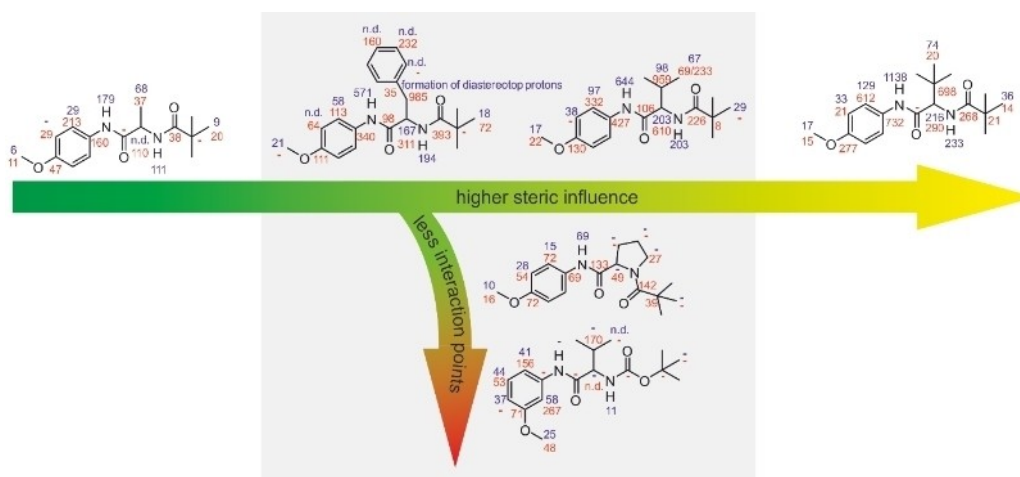


**Figure 3.** Splitting of signals (Proton: blue, Carbon: red) of compounds **1 b**, **2 c–g** at an enantiomeric ratio of 90:10. Compounds were dissolved in  $\text{CDCl}_3$ .

atoms. It can be observed that the splitting of the signals increases in spatial proximity to the stereogenic center. The exception is the carbonyl carbon atom of the amino acid. Similarly, distant atoms on the aromatic, methoxy and tert-butyl groups show little to no splitting. In contrast, particularly impressive values were observed for the splitting at the stereogenic center (up to 255 ppb for the proton signal and 822 ppb for the C signal of the amino acid's stereogenic center), the isopropyl group (C signal up to 1132 ppb) and the amide proton at the anisidine (up to 644 ppb).

Since the effect of splitting is most pronounced in the region of the stereogenic center, this indicates that the choice of amino acid used may also be of great importance. For this purpose, alanine, phenylalanine, *tert*-leucine and proline derivatives were tested. In combination with proline, which in contrast to the other applied amino acids was converted to a tertiary pivalic acid amide. In addition, an amide carbamate was investigated as a further functional group in the form of the Boc-protected amino acid (compounds **1**).

The use of small residues at the stereogenic center such as a methyl group in the case of the alanine derivative **2 d** leads to a significant reduction of the splitting ( $\Delta\delta_{\text{H}}(\text{NH at anisidine}) = 179$  ppb). Increasing steric demand at phenylalanine **2 f** ( $\Delta\delta_{\text{H}}(\text{NH at anisidine}) = 571$  ppb) and valine **2 c** ( $\Delta\delta_{\text{H}}(\text{NH at anisidine}) = 644$  ppb) increases the splitting behavior as well. With  $\Delta\delta_{\text{H}}(\text{NH at anisidine}) = 1138$  ppb, the value for *tert*-leucine **2 e** reaches the highest splitting (Figure 3). It was also observed that two secondary amides are required for successful recognition. Both the tertiary amide by using proline **2 g** ( $\Delta\delta_{\text{H}}(\text{NH at anisidine}) = 69$  ppb) and the carbamate (**1 b** instead of an amide ( $\Delta\delta_{\text{H}}(\text{NH at anisidine}) = \text{no splitting}$ ) lead to a significant reduction of the effect. This suggests that the three-point interaction is essential for the recognition.

The analysis of the amide protons of the enantiomerically pure compounds is also informative, since a small field shift is accompanied by a stronger hydrogen bond (Table 1). Particularly noteworthy is the comparatively low chemical shift of the amide protons for compounds **1 b** and **2 a** with 8.39 ppm for **1 b**

**Table 1.** Comparison of the chemical shift of the amide-/carbamate proton (compared compounds **1 b** and **2 a–g**).

Compound	Chemical shift NH at anisidine [ppm]	Chemical shift NH at amino acid [ppm]
<b>1 b</b>	8.39	5.20 (Carbamate)
<b>2 a</b>	8.10	6.33
<b>2 b</b>	8.80	6.47
<b>2 c</b>	8.75	6.50
<b>2 d</b>	9.02	6.57
<b>2 e</b>	8.82	6.52
<b>2 f</b>	8.47	6.54

and 8.10 ppm and 6.33 ppm for **2 a**, respectively. Both show no (**2 a**) or little (**1 b**) SIDA effect, which is very much in agreement with the observed shifts and associated weaker hydrogen bonds. Relatively strong low field shifts are observed for compounds **2 b–f** with values ranging from 8.47 to 9.02 ppm and 6.47 to 6.57 ppm, respectively. With a peak value of 9.14 ppm for the amide signal of **2 g**, the lack of a second hydrogen bond is partially compensated, leading to a weak SIDA effect.

In the context of aggregate formation, crystal structures of the pure (*S*)-enantiomer and the racemic mixture of **2 c** were comparatively crystallized, measured, and solved (Figure 4). Interestingly, the molecules of the racemate arrange in antiparallel pairs in the crystal, fixed by two hydrogen bonds (2.032 Å) (Figure 4C). Pairwise arrangement is also observed for the racemic mixture of phenylalanine derivative **2 f**. In contrast, crystallization of the enantiomerically pure compound results in a helical chain of monomers (Figure 4A and B). The rotation per molecule is 90°, and the pitch is 3.474 Å and 17.372 Å per complete rotation, respectively.

The helical structure is stabilized by two hydrogen bonds with 2.037 Å (NH-anisidine – C(O)-valine) and 2.189 Å (NH-valine – C(O)-piv) and a CH- $\pi$  interaction (distance proton to aromatic plane: 2.707 Å). Spatial proximity of the *tert*-butyl group as well

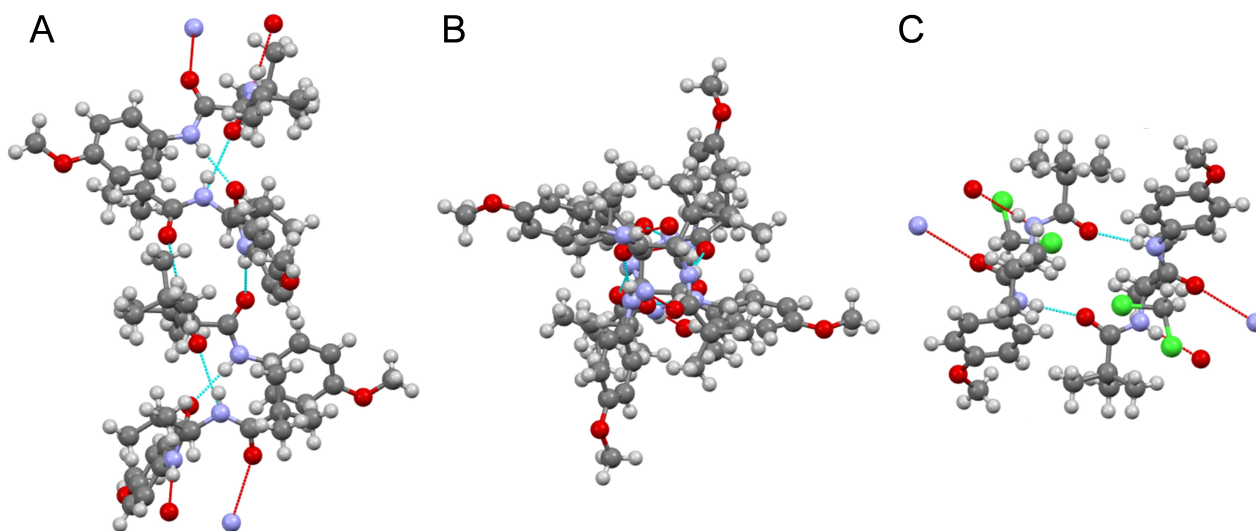


**Figure 4.** Crystal structures showing the packing of (*R*)-*N*-(4-methoxyphenyl)-3-methyl-2-pivalamidobutanamide (**R**-**2c**) from the side (A) and from top (B) in a helical chain stabilized by two hydrogen bonds and a CH- $\pi$  interaction, and (*R/S*)-*N*-(4-methoxyphenyl)-3-methyl-2-pivalamidobutanamide (**R/S**-**2c**) (C) as antiparallel pairs fixed by two hydrogen bonds. Carbon: gray; hydrogen: white; nitrogen: blue; oxygen: red; chlorine: green.

as the aromatic sites can also be detected by  $^1\text{H}$ -NOESY NMR experiments (see Figures S19 and S20 in the Supplementary Information). For this purpose,  $^1\text{H}$ -NOESY NMR experiments were carried out using the pseudo homomers (**R**-**2b** and (**R**-**2d** and the pseudo enantiomers (**R**-**2b** and (**S**-**2d**). Cross peaks were observed in both samples. The antiparallel orientation of the pseudo racemate results in a higher spatial proximity of the tert-butyl and the aryl group of the enantiomeric pairs and is in excellent agreement with the crystal structure.

For the proline derivative **2g**, no three-point interaction of the enantiomerically pure compound could be detected in the crystal. Hence, no helical arrangement was found. Instead, the formation of trimers is observed, which are linked to each other by only one hydrogen with 2.115 Å and 2.163 Å, respectively.

The variation of the temperature influences especially the amide protons. A decrease in temperature causes a deep field shift in the amide protons due to stronger hydrogen bonds. However, this has a different effect on the two sets of signals. The signal of the smaller population, which is primarily influenced by heterodimer formation, is less affected than that of the larger one (mainly homodimer formation).

In addition to these mechanistic studies, the SIDA effect was investigated in terms of its limitations. Half-concentrated solution of **2c** (33 mM) leads to slight reduction of the splitting. Despite high dilution at 1 mM of **2c**, the effect can still be observed, but significantly reduced. Nevertheless, at an enantiomeric ratio of 80:20, a splitting of 136 ppb appeared for the proton at the stereogenic center, 23 ppb for the tert-butyl- and 5 ppb for the methoxy group. In addition to the high dilution potential, the enormous sensitivity to the smallest enantiomer ratios is also worth mentioning (Figure 5). For **2c**, partial signal splitting was observed at 50.5:49.5 (1%ee) for the amide proton at the anisidine. Higher enantiomeric excesses lead to the splitting of further signals.

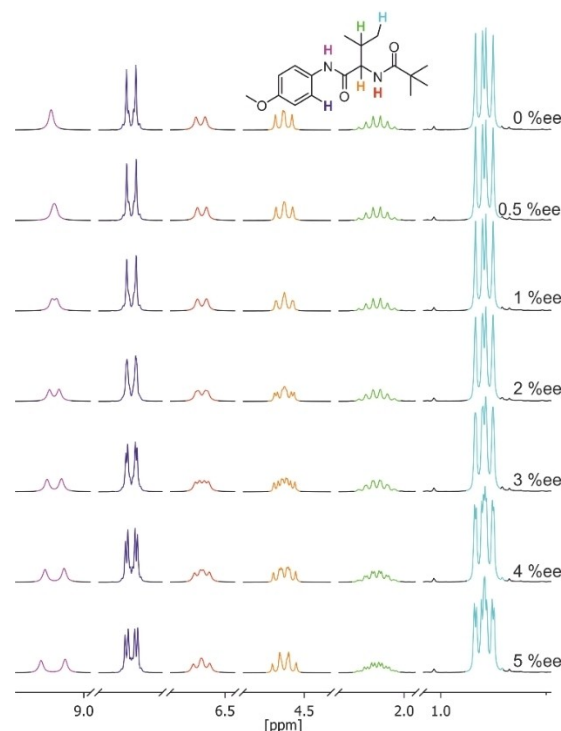


**Figure 5.** Section of the  $^1\text{H}$  NMR spectrum of compound **2c** in  $\text{CDCl}_3$  at different enantiomeric excesses.

By forming hydrogen bonds, it should be possible to differentiate enantiomers of chiral compounds that are also capable of forming hydrogen bonds but do not themselves exhibit a SIDA effect by NMR spectroscopy. As an example, racemic thalidomide was mixed with **2e** as a chiral shift reagent. This resulted in a uniform signal splitting of the imide proton in the  $^1\text{H}$  NMR spectrum (Figure 6 A). In addition to the racemic thalidomide,<sup>[57,58]</sup> different enantiomeric ratios of **2a** were also spiked with 30% of **2e** (Figure 6 B) causing a splitting

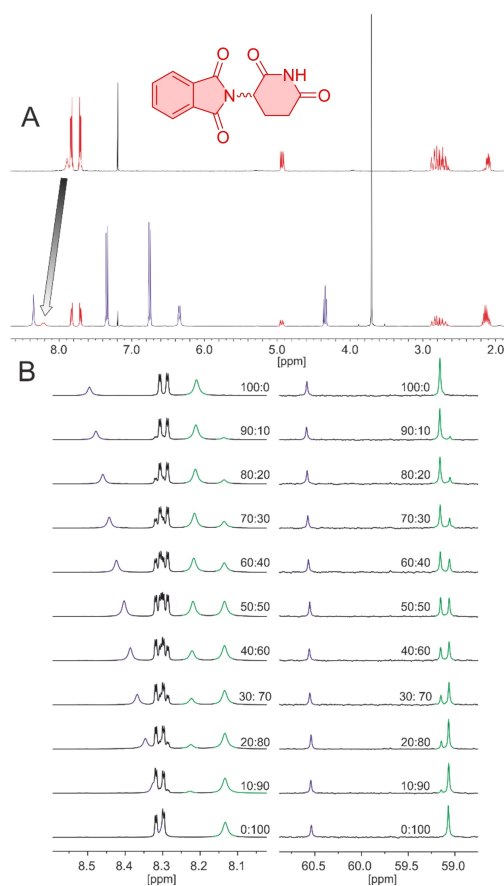


**Figure 6.** **2e** as chiral shift reagent. A)  $^1\text{H}$  NMR of a mixture of **2e** (blue signals) with thalidomide (red signals). This leads to a high field shift and splitting of the thalidomide imide signal. B) Section of  $^1\text{H}$  NMR (left) and  $^{13}\text{C}\{^1\text{H}\}$  (right) of a mixture of **2e** (blue signal) with **2a** (green signal) at a ratio of 30:70. The addition of **2e** leads to a baseline separated cleavage of the otherwise 'SIDA-inactive' **2a** and allows determination of the enantiomeric ratio of thalidomide.

of the previously SIDA-inactive **2a**. Exclusive signals in the  $^1\text{H}$  and  $^{13}\text{C}\{^1\text{H}\}$  spectra can thus be integrated and the enantiomeric ratio of **2a** determined.

## Conclusions

In the present study, a diamide-based compound class was presented that exhibits an enormous SIDA effect. The limitation of the effect, especially with respect to the functional groups (carbamate and tertiary amide), was investigated and the strength of the effect was increased enormously by specific manipulation. A splitting of the signals could be increased up to 1138 ppb at a ratio of 90:10. Likewise, the effect can be detected even at extremely low enantiomeric excesses. A plausible mechanism (helical chain vs. dimerization) of aggregate formation could be presented by means of crystal structures and  $^1\text{H}^1\text{H}$ -NOESY NMR experiments. Finally, the effect was used to determine enantiomeric ratios for 'SIDA-inactive' compounds. In the future, the here gained insights are of

particular importance for the design of supramolecular-based catalysts and materials.

## Experimental Section

**Materials.** Syntheses were carried out under an argon atmosphere (Ar 5.0) under exclusion of air. All glassware was flame-dried prior to use and standard Schlenk techniques were applied. THF (without stabilizer), toluene, diethylether, pentane and DCM were dried in an MB SPS-800 system and stored under argon. All chemicals were obtained from Sigma-Aldrich, abcr, Alfa Aesar, TCI Chemicals, Apollo Scientific, Fisher Scientific, Fluorochem or Carbosynth unless otherwise stated and used without further purification.

**General amide synthesis procedure A (GP A).** In a flame dried Schlenk flask under argon, the Boc-protected amino acid was dissolved in anhydrous DCM (0.1 M of anisidine). Anhydrous DIPEA and COMU were added at  $0^\circ\text{C}$ . After 15 min the anisidine was added in one portion. The reaction mixture was stirred overnight and allowed to warm up to room temperature. Subsequently, all volatiles were removed in under reduced pressure. The crude mixture was dissolved in EtOAc, washed with HCl (aq, 2 M, three times), saturated  $\text{NaHCO}_3$  (three times), water (three times) and brine (three times), dried over  $\text{Na}_2\text{SO}_4$  and all volatiles were removed under reduced pressure. The crude product was purified with one of three methods: 1.) flash chromatography (silica, DCM  $\rightarrow$  DCM:MeOH(1 %)), 2.) precipitated from DCM with diethyl ether or 3.) *n*-pentane.

**General amide synthesis procedure B (GP B).** The Boc-protected amino acid derivate was dissolved in chloroform and HCl (*i*PrOH, 5 M) was added at room temperature. The reaction was stirred overnight. Subsequently, all volatiles were removed under reduced pressure using a cooling trap. Then the mixture was dissolved in anhydrous DCM. DIPEA and pivaloyl chloride were added at  $0^\circ\text{C}$  and stirred overnight. The reaction mixture was diluted with DCM and washed with HCl (aq, 2 M, three times), saturated  $\text{NaHCO}_3$  (three times), water (three times) and brine (three times), dried over  $\text{Na}_2\text{SO}_4$  and all volatiles were removed under reduced pressure. The crude product was purified with flash chromatography (silica, DCM  $\rightarrow$  DCM:MeOH(1 %)).

According to GP B, **1a** (2.00 g, 6.20 mmol, 1.00 eq.), HCl (18.6 mL, 93.1 mL, 15 eq.) and after evaporation DIPEA (5.00 eq.) and pivaloyl chloride (2.50 eq.) was used. **2a** was obtained as off-white solid (1.23 g, 1.23 mmol, 12 %).

**NMR spectroscopy.** NMR-spectra were recorded on Varian NMR-System (300, 400 and 600 MHz) and Bruker Avance III HD and DRX (300, 400 and 800 MHz) spectrometers. Chemical shifts are reported in ppm, coupling constants *J* in Hz and peak multiplicity is defined by *s* (singlet), *d* (doublet), *t* (triplet), *q* (quartet) and *m* (multiplet). The solvent residual signals were used as internal standards. Structural assignments were made with additional information from gCOSY, gHSQC, and gHMBC experiments. The numbering is depicted in the respective figure shown above each procedure.

**NMR titration experiments.** A stock solution of each enantiomerically pure compound was prepared in  $\text{CDCl}_3$  (67 mM). For the titration experiment the corresponding amount of each enantiomer was transferred with a Hamilton precision syringe into an NMR tube. After gently shaking by hand the sample was put into the autosampler of the NMR instrument and the measurement was carried out.

For  $^1\text{H}$  NMR experiments the following parameters were applied:

- $\rightarrow$  number of scans: 32
- $\rightarrow$  relaxation delay: 0.1 s

→ acquisition time: 4.0 s  
 → pulse width: 3.4  $\mu$ s  
 For  $^{13}\text{C}$  NMR experiments the following parameters were applied:  
 number of scans: 2048/4096  
 → relaxation delay: 0.1 s  
 → acquisition time: 3.6 s  
 → pulse width: 4.6  $\mu$ s

**Mass spectrometry.** Mass spectrometric measurements were performed on Thermo Finnigan LTQ FT Ultra FT-ICR (ESI). Infrared spectra were recorded on a Thermo Scientific Nicolet 6700 ATR-FT-IR spectrometer.

**Single crystal X-ray diffraction crystallography.** Crystallographic data was collected on Bruker D8 Venture TX with Mo  $K\alpha$  radiation ( $\lambda = 0.71073 \text{ \AA}$ ). Deposition Numbers 2333016 (for **(R)**-2c), 2333017 (for *rac*-2c), 2333018 (for **(R)**-2g) contain the supplementary crystallographic data for this paper. These data are provided free of charge by the joint Cambridge Crystallographic Data Centre and Fachinformationszentrum Karlsruhe.

**HPLC, HPLC-MS, GC, and GC-MS measurements.** HPLC measurements were performed on an Agilent Technologies 1200 HPLC (Agilent Technologies, Palo Alto, California, USA), equipped with a binary solvent pump, an autosampler, membrane solvent degasser, DAD detector and a quadrupole mass spectrometer Agilent 6120, equipped with an APCI source. All operations were controlled by the Agilent ChemStation software (Agilent Technologies, Palo Alto, California, USA). The solvents used were obtained from Sigma-Aldrich (HPLC-grade quality). Gas chromatographic separations were performed on a Thermo Trace ISQ GC-MS equipped with an autosampler/ split injector (250 °C), a flame-ionization detector (250 °C) and a quadrupole MS (Thermo, San Jose, California, U.S.A.). Electron impact mass spectra (EI-MS, ion source temperature 200 °C) were recorded at an electron energy of 70 eV.

## Acknowledgements

We acknowledge financial support from the Ludwig-Maximilians-University Munich. We thank Dr. Peter Mayer (Department of Chemistry, LMU München) for the X-ray structure determination. Open Access funding enabled and organized by Projekt DEAL.

## Conflict of Interests

The authors declare no conflict of interest.

## Data Availability Statement

The data that support the findings of this study are available in the supplementary material of this article.

**Keywords:** SIDA · NMR spectroscopy · supramolecular chemistry · recognition · chirality

- [1] D. A. Leigh, *Angew. Chem. Int. Ed.* **2016**, *55*, 14506–14508.  
 [2] S. J. Wezenberg, B. L. Feringa, *Nat. Commun.* **2018**, *9*, 1984.

- [3] J. Chen, F. K. -C. Leung, M. C. A. Stuart, T. Kajitani, T. Fukushima, E. V. D. Giessen, B. L. Feringa, *Nat. Chem.* **2018**, *10*, 132–138.  
 [4] Y. Deng, Q. Zhang, B. L. Feringa, H. Tian, D. -H. Qu, *Angew. Chem. Int. Ed.* **2020**, *59*, 5278–5283.  
 [5] D. J. van Dijken, J. M. Beierle, M. C. A. Stuart, W. Szymański, W. R. Browne, B. L. Feringa, *Angew. Chem. Int. Ed.* **2014**, *53*, 5073–5077.  
 [6] G. Gil-Ramírez, D. A. Leigh, A. J. Stephens, *Angew. Chem. Int. Ed.* **2015**, *54*, 6110–6150.  
 [7] J. Zhong, L. Zhang, D. P. August, G. F. S. Whitehead, D. A. Leigh, *J. Am. Chem. Soc.* **2019**, *141*, 14249–14256.  
 [8] S. Erbas-Cakmak, S. D. P. Fielden, U. Karaca, D. A. Leigh, C. T. McErnan, D. J. Tetlow, M. R. Wilson, *Science* **2017**, *358*, 340–343.  
 [9] T. Iseki, M. F. J. Mabesoone, M. A. J. Koenis, B. A. G. Lamers, E. Weyandt, L. N. J. D. Windt, W. J. Buma, A. R. A. Palmans, E. W. Meijer, *Chem. Sci.* **2021**, *12*, 13001–13012.  
 [10] M. L. Ślęczkowski, M. F. J. Mabesoone, P. Ślęczkowski, A. R. A. Palmans, E. W. Meijer, *Nat. Chem.* **2021**, *13*, 200–207.  
 [11] A. Das, G. Vantomme, A. J. Markvoort, H. M. M. T. Eikelder, M. Garcia-Iglesias, A. R. A. Palmans, E. W. Meijer, *J. Am. Chem. Soc.* **2017**, *139*, 7036–7044.  
 [12] D. Bindl, E. Heinemann, P. K. Mandal, I. Huc, *Chem. Commun.* **2021**, *57*, 5662–5665.  
 [13] D. Bindl, P. K. Mandal, L. Allmendinger, I. Huc, *Angew. Chem. Int. Ed.* **2022**, *61*, e202116509.  
 [14] P. Aoun, A. Hammoud, M. A. Martínez-Aguirre, L. Bouteiller, M. Raynal, *Catal. Sci. Technol.* **2022**, *12*, 834–842.  
 [15] M. A. Martínez-Aguirre, Y. Li, N. Vanthuyne, L. Bouteiller, M. Raynal, *Angew. Chem. Int. Ed.* **2021**, *60*, 4183–4191.  
 [16] J. M. Zimbron, X. Caumes, Y. Li, C. M. Thomas, M. Raynal, L. Bouteiller, *Angew. Chem. Int. Ed.* **2017**, *56*, 14016–14019.  
 [17] R. Wechsel, M. Žabka, J. W. Ward, J. Clayden, *J. Am. Chem. Soc.* **2018**, *140*, 3528–3531.  
 [18] L. Byrne, J. Solà, T. Boddaert, T. Marcelli, R. W. Adams, G. A. Morris, J. Clayden, *Angew. Chem. Int. Ed.* **2014**, *53*, 151–155.  
 [19] J. Solà, S. Fletcher, A. Castellanos, J. Clayden, *Angew. Chem. Int. Ed.* **2010**, *49*, 6836–6839.  
 [20] G. Lautrette, B. Wicher, B. Kauffmann, Y. Ferrand, I. Huc, *J. Am. Chem. Soc.* **2016**, *138*, 10314–10322.  
 [21] P. Mateus, N. Chandramouli, C. D. Mackereth, B. Kauffmann, Y. Ferrand, I. Huc, *Angew. Chem. Int. Ed.* **2020**, *59*, 5797–5805.  
 [22] S. Saha, B. Kauffmann, Y. Ferrand, I. Huc, *Angew. Chem. Int. Ed.* **2018**, *57*, 13542–13546.  
 [23] G. Storch, O. Trapp, *Nat. Chem.* **2017**, *9*, 179–187.  
 [24] J. F. Scholtes, O. Trapp, *Angew. Chem. Int. Ed.* **2019**, *58*, 6306–6310.  
 [25] J. F. Scholtes, O. Trapp, *Chem. Eur. J.* **2019**, *25*, 11707–11714.  
 [26] J. F. Scholtes, O. Trapp, *Organometallics* **2019**, *38*, 3955–3960.  
 [27] K. C. Cundy, P. A. Crooks, *J. Chromatogr.* **1983**, *281*, 17–33.  
 [28] O. Trapp, V. Schurig, *Tetrahedron: Asymmetry* **2010**, *21*, 1334–1340.  
 [29] Y. Suzuki, J. Han, O. Kitagawa, J. L. Aceña, K. D. Klika, V. A. Soloshonok, *RSC Adv.* **2015**, *5*, 2988–2993.  
 [30] A. Wzorek, K. D. Klika, J. Drabowicz, A. Sato, J. L. Aceña, V. A. Soloshonok, *Org. Biomol. Chem.* **2014**, *12*, 4738–4746.  
 [31] A. E. Sorochinsky, T. Katagiri, T. Ono, A. Wzorek, J. L. Aceña, V. A. Soloshonok, *Chirality* **2013**, *25*, 365–368.  
 [32] V. A. Soloshonok, C. Roussel, O. Kitagawa, A. E. Sorochinsky, *Chem. Soc. Rev.* **2012**, *41*, 4180–4188.  
 [33] J. Martens, R. Bhushan, *Helv. Chim. Acta* **2014**, *97*, 161–187.  
 [34] M. Maeno, E. Tokunaga, T. Yamamoto, T. Suzuki, Y. Ogino, E. Ito, M. Shiro, T. Asahi, N. Shibata, *Chem. Sci.* **2015**, *6*, 1043–1048.  
 [35] V. Dašková, D. Padín, B. L. Feringa, *J. Am. Chem. Soc.* **2022**, *144*, 23603–23613.  
 [36] J. A. Dale, D. L. Dull, H. S. Mosher, *J. Org. Chem.* **1969**, *34*, 2543–2549.  
 [37] W. H. Pirkle, D. L. Sikkenga, M. S. Pavlin, *J. Org. Chem.* **1977**, *42*, 384–387.  
 [38] A. B. Ouryupin, M. I. Kadyko, P. V. Petrovskii, E. I. Fedin, *Chirality* **1994**, *6*, 1–4.  
 [39] F. Aiello, G. U. Barretta, F. Balzano, F. Spiaggia, *Molecules* **2023**, *28*, 6854.  
 [40] Martin J. P. Harger, *J. Chem. Soc. Chem. Commun.* **1976**, 555–556.  
 [41] Martin J. P. Harger, *J. Chem. Soc. Perkin Trans. 2* **1978**, 326–331.  
 [42] Martin J. P. Harger, *J. Chem. Soc. Perkin Trans. 2* **1980**, 154–160.  
 [43] M. M. Safont-Sempere, P. Osswald, M. Stölte, M. Grüne, M. Renz, M. Kaupp, K. Radacki, H. Braunschweig, F. Würthner, *J. Am. Chem. Soc.* **2011**, *133*, 9580–9591.  
 [44] S. D. Bergman, M. Kol, *Inorg. Chem.* **2005**, *44*, 1647–1654.  
 [45] Z. Xu, Q. Wang, J. Zhu, *J. Am. Chem. Soc.* **2015**, *137*, 6712–6724.  
 [46] A. Horeau, J. P. Guetté, *Tetrahedron* **1974**, *30*, 1923–1931.

- [47] S. K. Ghosh, *J. Pept. Res.* **1999**, *53*, 261–274.
- [48] M. I. Kabachnik, T. A. Mastryukova, E. I. Fedin, M. S. Vaisberg, L. L. Morozov, P. V. Petrovsky, A. E. Shipov, *Tetrahedron* **1976**, *32*, 1719–1728.
- [49] B. S. Jursic, S. I. Goldberg, *J. Org. Chem.* **1992**, *57*, 7172–7174.
- [50] A. Dobashi, N. Saito, Y. Motoyama, S. Hara, *J. Am. Chem. Soc.* **1986**, *108*, 307–308.
- [51] C. Luchinat, S. Roelens, *J. Am. Chem. Soc.* **1986**, *108*, 4873–4878.
- [52] C. Giordano, A. Restelli, M. Villa, R. Annunziata, *J. Org. Chem.* **1991**, *56*, 2270–2272.
- [53] G. Storch, M. Haas, O. Trapp, *Chem. Eur. J.* **2017**, *23*, 5414–5418.
- [54] J. F. Scholtes, O. Trapp, *Synlett* **2021**, *32*, 971–980.
- [55] L. C. Mayer, S. Heitsch, O. Trapp, *Acc. Chem. Res.* **2022**, *55*, 3345–3361.
- [56] M. I. Kabachnik, T. A. Mastryukova, E. I. Fedin, M. S. Vaisberg, L. L. Morozov, P. V. Petrovskii, A. E. Shipov, *Russ. Chem. Rev.* **1978**, *47*, 821.
- [57] M. Mayering, B. Chankvetadze, G. Blaschke, *J. Chromatogr. A* **2000**, *876*, 157–167.
- [58] O. Trapp, G. Schoetz, V. Schurig, *J. Pharm. Biomed. Anal.* **2002**, *27*, 497–505.

---

Manuscript received: February 15, 2024

Accepted manuscript online: April 24, 2024

Version of record online: June 10, 2024